2024 IEEE 63rd Conference on Decision and Control (CDC)
December 16-19, 2024. MiCo, Milan, Italy

Fixed-Time Fault-Tolerant Control of Robotic Manipulators with Actuator Faults Based on Fixed-Time Extended State Observer

Xing Ren, Jiange Kou, Yuanchao Cao, Qing Guo, *Senior Member*,
Zhenlei Chen, Yan Shi, Tieshan Li, *Senior Member*

***Abstract*— This paper proposes a fixed-time fault-tolerant controller for n-DOF robotic manipulators with actuator partial loss of effectiveness (LOE) faults, external disturbances, and unknown nonlinearities. A novel fixed-time extended state observer (FxTESO) is designed to estimate joint velocities and lumped uncertainty, and the estimation error can theoretically be arbitrarily small by increasing the bandwidth. An adaptive law is designed to estimate an upper bound related to FxTESO error, which can enhance the controller robustness. The proposed controller can guarantee practical fixed-time stability of the manipulator, and require no velocity measurement and prior information about lumped uncertainty. The comparative experiments with the other state-of-the-art controllers on a 4-DOF manipulator under different external disturbances and actuator faults verify the superiority of the proposed controller.**

I. Introduction

Nowadays, robotic manipulators have made significant contributions to various fields, such as industrial manufacturing, healthcare, and aerospace, etc. Therefore, high-accuracy control, strong reliability, and fast response speed are crucial for manipulators. However, due to the complex structure and dynamic working environment, the manipulators are often affected by unknown nonlinearities and external disturbances. Many studies have been conducted on these issues, such as in [1], a sliding mode disturbance observer is designed to compensate for uncertainty and disturbance. In [2], the RBF neural network are used to estimate the unknown manipulator dynamics and external disturbance to address their negative effects. In [3], two adaptive laws are designed to estimate the uncertain kinematics and uncertain dynamics of the manipulator respectively, and the developed controller can guarantee that the estimation error and tracking error converge globally exponentially.

The aforementioned studies only consider the effects of uncertainties and disturbances, without considering the issue of faults. However, manipulators are often used for high-load or high-frequency tasks, which can easily lead to actuator faults such as partial loss of effectiveness (LOE) faults, bias faults, or stuck faults, etc. Fault-tolerant control (FTC) is an effective strategy for handling system faults. For example, in [4], an FTC controller based on adaptive fuzzy integral sliding mode control is developed, and a hybrid fuzzy approximation and disturbance observer is designed to estimate the actuator faults. In [5], a learning-based adaptive FTC method is proposed, which utilizes RBF networks to identify system uncertainties and actuator faults. In [6], a fault diagnosis based on time delay estimation (TDE) is proposed, and developed an FTC controller by combining TDE-based fault diagnosis, nonsingular fast terminal sliding mode control (NFTSMC), and high-order sliding mode control.

However, these approaches only guarantee that the system states are uniformly ultimately bounded (UUB) or finite time convergence, and the settling time is related to the initial conditions. Therefore, fixed-time control is proposed [7] to ensure that the system states can converge within a fixed time constant, and the settling time is independent of the initial conditions. There have been some studies on fixed-time control of manipulators, such as fixed-time neural network control [8], fixed-time adaptive fuzzy control [9], and reinforcement learning-based fixed-time control [10], etc. Fixed-time FTC of manipulators has also been studied by researchers [11], [12]. In addition, most robotic manipulator controllers require joint velocity, but in practice, manipulators may not be equipped with velocity sensors, and the approximate velocity obtained by differentiating the position signal will be affected by noise [13]. Extended state observer (ESO) can estimate both unmeasured states and disturbances of the system simultaneously. Besides, fixed-time ESO (FxTESO) has also been proposed to guarantee that the estimation errors converge within a fixed time [14].

Inspired by the aforementioned studies and issues, this paper proposes a FxTESO-based fixed-time fault-tolerant controller for manipulators with actuator partial LOE faults, external disturbances, and unknown nonlinearities. The main contributions are as follows:

1) In this paper, a novel FxTESO is designed to estimate the joint velocities and lumped uncertainty of the manipulator. The estimation errors can achieve fixed time convergence, and the errors can be reduced by increasing the bandwidth ω_o of FxTESO.
2) The proposed controller can guarantee that the tracking error of each joint converges to a neighborhood of zero

This work is supported by National Natural Science Foundation of China (No 52175046, 52305054, and 51939001), Sichuan Science and Technology Program (No. 24ZDYF0070), and China Postdoctoral Science Foundation (No. 2022M720024). The corresponding author is *Q. Guo*.

X. Ren, Z. Chen, and T. Li are with the School of Automation Engineering, University of Electronic Science and Technology of China, Chengdu 611130, China (e-mail: renxing@std.uestc.edu.cn, zhenlei_chen@std.uestc.edu.cn, litieshan073@uestc.edu.cn).

J. Kou and Y. Shi are with the School of Automation Science and Electrical Engineering, Beihang University (BUAA), Beijing 100191, China (e-mail: koujiange@buaa.edu.cn, shiyan@buaa.edu.cn).

Y. Cao and Q. Guo are with the School of Aeronautics and Astronautics, University of Electronic Science and Technology of China, Chengdu 611130, China (e-mail: yc.cao@std.uestc.edu.cn, guoqinguestc@uestc.edu.cn).

within a fixed time, and the settling time is independent of the initial conditions. An adaptive law is designed to estimate an upper bound related to the estimation error of FxTESO, which can enhance the robustness of the controller.

3) The controller proposed in this paper uses estimated joint velocities, eliminating the need for velocity sensors, and avoiding additional significant noise generated by differentiating the position signal. In addition, the proposed controller requires no prior information about the lumped uncertainty.

II. Problem Formulation and Preliminaries

A. Model of Robotic Manipulator

The dynamic model of a class of rigid manipulator with n-links is constructed as

$$\begin{aligned}\ddot{\mathbf{q}} &= \mathbf{M}^{-1}(\mathbf{q})\boldsymbol{\tau} + \mathbf{M}^{-1}(\mathbf{q})\left((\boldsymbol{\Lambda}-\mathbf{I}_n)\boldsymbol{\tau} - \mathbf{C}(\mathbf{q},\dot{\mathbf{q}})\dot{\mathbf{q}}\right) \\ &\quad + \mathbf{M}^{-1}(\mathbf{q})\left(-\mathbf{G}(\mathbf{q}) - \mathbf{F}(\dot{\mathbf{q}}) - \boldsymbol{\tau}_d - \boldsymbol{\Delta}\right) \\ &= \mathbf{M}^{-1}(\mathbf{q})\boldsymbol{\tau} + \mathbf{d}(t)\end{aligned} \tag{1}$$

where $\mathbf{q}, \dot{\mathbf{q}}, \ddot{\mathbf{q}} \in \mathbb{R}^n$ are the position, velocity, and acceleration of the joints, $\boldsymbol{\tau} \in \mathbb{R}^n$ is the driving torque, $\mathbf{M}(\mathbf{q}) \in \mathbb{R}^{n\times n}$ is the inertia matrix, $\mathbf{C}(\mathbf{q},\dot{\mathbf{q}})$ is the Centripetal and Coriolis matrix, $\mathbf{G}(\mathbf{q})$ is the vector of gravitational torque, and $\mathbf{F}(\dot{\mathbf{q}})$ is the friction vector. In addition, $\boldsymbol{\Lambda} = \mathrm{diag}\{\lambda_i\}$ is the matrix of the actuator LOE fault coefficients with $\lambda_i \in (0,1]$, $\mathbf{I}_n$ is the identity matrix, $\boldsymbol{\tau}_d$ is the external disturbances, $\boldsymbol{\Delta} = \Delta\mathbf{M}\ddot{\mathbf{q}} + \Delta\mathbf{C}\dot{\mathbf{q}} + \Delta\mathbf{G}$ is the model uncertainty. Matrix $\mathbf{C}(\mathbf{q},\dot{\mathbf{q}})$, vectors $\mathbf{G}(\mathbf{q})$, $\mathbf{F}(\mathbf{q})$ and $\boldsymbol{\Delta}$ are difficult to obtain, thus the lumped uncertainty $\mathbf{d}(t) = [d_1(t),\cdots,d_n(t)]^T$ contains actuator fault components, external disturbances, and unknown nonlinearities.

Assumption 1 : The lumped uncertainty $\mathbf{d}(t)$ and its derivative $\dot{\mathbf{d}}(t)$ are bounded, such that $\|\mathbf{d}(t)\| \le \bar{d}$ and $\left\|\dot{\mathbf{d}}(t)\right\| \le \bar{\gamma}$, where $\bar{d}$ and $\bar{\gamma}$ are unknown positive constants.

B. Preliminaries

Definition 1 [15]: A function F is homogeneous of degree d with respect to the weights $(r_1,\cdots,r_n) \in \mathbb{R}^n_{>0}$ if $F(\rho^{r_1}x_1,\cdots,\rho^{r_n}x_n) = \rho^d F(x_1,\cdots,x_n)$ for all $\rho > 0$.

A vector field $\mathbf{v}$ is homogeneous of degree d with respect to the weights $(r_1,\cdots,r_n) \in \mathbb{R}^n_{>0}$ if the ith component v_i of $\mathbf{v}$ satisfies $v_i(\rho^{r_1}x_1,\cdots,\rho^{r_n}x_n) = \rho^{r_i+d}v_i(x_1,\cdots,x_n)$ for all $1 \le i \le n$ and $\rho > 0$.

Lemma 1 [14]: If continuous functions $F_1(\mathbf{x}) > 0$ and $F_2(\mathbf{x})$, $\mathbf{x} \in \mathbb{R}^n$, are homogeneous with respect to $\mathbf{r}$ of degree $l_1 > 0$ and $l_2 > 0$, there exists

$$\vartheta_1[F_1(\mathbf{x})]^{\frac{l_2}{l_1}} \le F_2(\mathbf{x}) \le \vartheta_2[F_1(\mathbf{x})]^{\frac{l_2}{l_1}} \tag{2}$$

where $\vartheta_1 = \min_{\{\mathbf{g}:F_1(\mathbf{g})=1\}}F_2(\mathbf{g})$ and $\vartheta_2 = \max_{\{\mathbf{g}:F_1(\mathbf{g})=1\}}F_2(\mathbf{g})$.

Lemma 2 [16]: If there exists a candidate Lyapunov function $V(\mathbf{x})$, $\mathbf{x} \in \mathbb{R}^n$, satisfies

$$\dot{V}(\mathbf{x}) \le -\alpha V^p(\mathbf{x}) - \beta V^q(\mathbf{x}) \tag{3}$$

where $\alpha > 0, \beta > 0, 0 < p < 1, q > 1$ are positive constants, then the origin of the system $\dot{\mathbf{x}} = f(\mathbf{x}(t))$ is fixed-time stable and the settling time T satisfies

$$T \le T_{\max} = \frac{1}{\alpha(1-p)} + \frac{1}{\beta(q-1)}. \tag{4}$$

If the following inequality holds:

$$\dot{V}(\mathbf{x}) \le -\alpha V^p(\mathbf{x}) - \beta V^q(\mathbf{x}) + \eta \tag{5}$$

where $0 < \eta < \infty$, then the trajectory of $\dot{\mathbf{x}} = f(\mathbf{x}(t))$ is practical fixed-time stable and the settling time T satisfies

$$T \le T_{\max} = \frac{1}{\alpha\phi(1-p)} + \frac{1}{\beta\phi(q-1)} \tag{6}$$

where $0 < \phi < 1$ is a positive constant, and the residual set of the solution is

$$\mathbf{x} \in \left\{ V(\mathbf{x}) \le \min\left\{ \left(\frac{\eta}{(1-\phi)\alpha}\right)^{\frac{1}{p}}, \left(\frac{\eta}{(1-\phi)\beta}\right)^{\frac{1}{q}} \right\} \right\}. \tag{7}$$

Lemma 3 [17]: For $\forall\vartheta,\chi$, and any positive constant ς, ι and ω, the following inequality holds:

$$|\vartheta|^{\varsigma}|\chi|^{\iota} \le \frac{\varsigma}{\varsigma+\iota}\omega|\vartheta|^{\varsigma+\iota} + \frac{\iota}{\varsigma+\iota}\omega^{\frac{-\varsigma}{\iota}}|\chi|^{\varsigma+\iota}. \tag{8}$$

Lemma 4 [18]: For $\forall x \ge y$, $c > 1$ and c is a odd number, the following inequality holds:

$$y(x-y)^c \le \frac{c}{c+1}\left(x^{c+1} - y^{c+1}\right). \tag{9}$$

Lemma 5 : For $\nu_i \in \mathbb{R}$, $i = 1,\cdots,n$, $0 < \beta_1 < 1$, and $\beta_2 > 1$, the following inequalities hold:

$$\left(\sum_{i=1}^n |\nu_i|\right)^{\beta_1} \le \sum_{i=1}^n |\nu_i|^{\beta_1}, \left(\sum_{i=1}^n |\nu_i|\right)^{\beta_2} \le n^{\beta_2-1}\sum_{i=1}^n |\nu_i|^{\beta_2}. \tag{10}$$

III. Main Results

A. Design of Fixed-Time Extended State Observer

The lumped uncertainty $\mathbf{d}(t)$ is defined as an extended state variable $\mathbf{x}_3$, and the derivative of $\mathbf{x}_3$ is $\dot{\mathbf{x}}_3 = \boldsymbol{\gamma}$, where $\boldsymbol{\gamma} = [\gamma_1,\cdots,\gamma_n]^T$ is an unknown function, then the states of the manipulator model are $\left[\mathbf{x}_1^T,\mathbf{x}_2^T,\mathbf{x}_3^T\right]^T = \left[\mathbf{q}^T,\dot{\mathbf{q}}^T,\mathbf{d}^T(t)\right]^T$. The FxTESO is designed as

$$\begin{cases}\dot{\hat{\mathbf{x}}}_1 = \hat{\mathbf{x}}_2 + g_1\omega_0\left(\mathbf{Sig}^{\alpha_1}(\tilde{\mathbf{x}}_1) + \mathbf{Sig}^{\beta_1}(\tilde{\mathbf{x}}_1)\right) \\ \dot{\hat{\mathbf{x}}}_2 = \hat{\mathbf{x}}_3 + g_2\omega_0^2\left(\mathbf{Sig}^{\alpha_2}(\tilde{\mathbf{x}}_1) + \mathbf{Sig}^{\beta_2}(\tilde{\mathbf{x}}_1)\right) + \mathbf{M}^{-1}\boldsymbol{\tau} \\ \dot{\hat{\mathbf{x}}}_3 = g_3\omega_0^3\left(\mathbf{Sig}^{\alpha_3}(\tilde{\mathbf{x}}_1) + \mathbf{Sig}^{\beta_3}(\tilde{\mathbf{x}}_1)\right)\end{cases} \tag{11}$$

where $\hat{\mathbf{x}}_j\,(j = 1,\cdots,3)$ is the state estimation, $\tilde{\mathbf{x}}_j = \mathbf{x}_j - \hat{\mathbf{x}}_j$ is the estimation error, g_j is the design gain, ω_0 is the bandwidth of the FxTESO, $\mathbf{Sig}^a(\mathbf{x}) = [sig^a(x_1),\cdots,sig^a(x_n)]^T$ with $sig^a(x) = \mathrm{sgn}(x)|x|^a$, $\alpha_j = j(\alpha-1)+1$, $\beta_j = 1/\alpha + (j-1)(\alpha-1)$, where $\alpha \in (1-\varepsilon_1, 1)$ and $\varepsilon_1 > 0$ is a small constant.

Theorem 1 : The state estimation error $\tilde{\mathbf{x}}_j = \mathbf{x}_j - \hat{\mathbf{x}}_j$ can converge to a neighborhood of the origin within a fixed

time, and the convergence domain can be arbitrarily small by increasing the bandwidth ω_0.

Proof: According to (1) and (11), the estimation error dynamics of the FxTESO can be described as

$$\begin{cases}\dot{\boldsymbol{\xi}}_1 = \omega_0\boldsymbol{\xi}_2 - g_1\omega_0\left(\mathbf{Sig}^{\alpha_1}\left(\boldsymbol{\xi}_1\right) + \mathbf{Sig}^{\beta_1}\left(\boldsymbol{\xi}_1\right)\right)\\ \dot{\boldsymbol{\xi}}_2 = \omega_0\boldsymbol{\xi}_3 - g_2\omega_0\left(\mathbf{Sig}^{\alpha_2}\left(\boldsymbol{\xi}_1\right) + \mathbf{Sig}^{\beta_2}\left(\boldsymbol{\xi}_1\right)\right)\\ \dot{\boldsymbol{\xi}}_3 = -g_3\omega_0\left(\mathbf{Sig}^{\alpha_3}\left(\boldsymbol{\xi}_1\right) + \mathbf{Sig}^{\beta_3}\left(\boldsymbol{\xi}_1\right)\right) + \boldsymbol{\gamma}/\omega_0^2\end{cases} \tag{12}$$

where $\boldsymbol{\xi} = \left[\boldsymbol{\xi}_1^T, \boldsymbol{\xi}_2^T, \boldsymbol{\xi}_3^T\right]^T = \left[\tilde{\mathbf{x}}_1^T, \tilde{\mathbf{x}}_2^T/\omega_0, \tilde{\mathbf{x}}_3^T/\omega_0^2\right]^T$, and $\boldsymbol{\xi}_j = \left[\xi_{j,1}, \cdots, \xi_{j,n}\right]^T$. Firstly, consider the following system:

$$\dot{\boldsymbol{\xi}} = \mathbf{S}_\alpha\left(\boldsymbol{\xi}\right) \tag{13}$$

where

$$\mathbf{S}_\alpha\left(\boldsymbol{\xi}\right) = \begin{bmatrix}\omega_0\boldsymbol{\xi}_2 - g_1\omega_0\mathbf{Sig}^{\alpha_1}\left(\boldsymbol{\xi}_1\right)\\ \omega_0\boldsymbol{\xi}_3 - g_2\omega_0\mathbf{Sig}^{\alpha_2}\left(\boldsymbol{\xi}_1\right)\\ -g_3\omega_0\mathbf{Sig}^{\alpha_3}\left(\boldsymbol{\xi}_1\right)\end{bmatrix}. \tag{14}$$

Define $\mathbf{v} = \left[\mathbf{v}_1^T, \cdots, \mathbf{v}_n^T\right]^T$ with $\mathbf{v}_i = \left[\xi_{1,i}, \cdots, \xi_{3,i}\right]^T (i = 1, \cdots, n)$. If $\alpha = 1$, the error system (13) can be written as $\dot{\mathbf{v}} = \omega_0\left(\mathbf{I}_n \otimes \mathbf{A}\right)\mathbf{v}$ with $\mathbf{A} = [-g_1, 1, 0; -g_2, 0, 1; -g_3, 0, 0]$, and $\otimes$ represents Kronecker product. If all gains are designed such that the matrix $\mathbf{A}$ is Hurwitz, then there exists a Lyapunov equation $\mathbf{PA} + \mathbf{A}^T\mathbf{P} = -\mathbf{Q}$, where $\mathbf{P}$ and $\mathbf{Q}$ are positive definite matrices, and $\mathbf{P}$ is symmetric. Consider the following candidate Lyapunov function:

$$V_1\left(\alpha, \boldsymbol{\xi}\right) = \mathbf{z}^T\left(\mathbf{I}_n \otimes \mathbf{P}\right)\mathbf{z} \tag{15}$$

where $\mathbf{z} = \left[\mathbf{z}_1^T, \cdots, \mathbf{z}_n^T\right]^T$ with $\mathbf{z}_i = f_z\left(\mathbf{v}_i\right) = \left[sig^{\frac{1}{\mu}}\left(\xi_{1,i}\right), sig^{\frac{1}{\mu\alpha_1}}\left(\xi_{2,i}\right), sig^{\frac{1}{\mu\alpha_2}}\left(\xi_{3,i}\right)\right]^T$, $\mu = \alpha_1\alpha_2\alpha_3$. According to *Definition 1*, the function $V_1\left(\alpha, \boldsymbol{\xi}\right)$ is homogeneous of degree $l_1 = 2/\mu$ with respect to weight $\mathbf{r} = (1, \alpha, 2\alpha - 1)$. The Lie derivative $L_{S_\alpha}V_1\left(\alpha, \boldsymbol{\xi}\right)$ of $V_1\left(\alpha, \boldsymbol{\xi}\right)$ along $\mathbf{S}_\alpha\left(\boldsymbol{\xi}\right)$ is homogeneous of degree $l_2 = 2/\mu + \alpha - 1$ with respect to $\mathbf{r}$. According to *Lemma 1* , there exists $\kappa_\alpha = -\max_{\{\boldsymbol{g}:V_1(\alpha,\boldsymbol{g})=1\}}L_{S_\alpha}V_1\left(\alpha, \boldsymbol{g}\right) > 0$ such that the following inequality holds:

$$L_{S_\alpha}V_1\left(\alpha, \boldsymbol{\xi}\right) \le -\kappa_\alpha V_1^{l_2/l_1} \tag{16}$$

where $\lim_{\alpha\to 1}\kappa_\alpha = \lambda_{\min}\left(\mathbf{Q}\right)/\lambda_{\max}\left(\mathbf{P}\right)$, $\lambda_{\min}\left(\cdot\right)$ and $\lambda_{\max}\left(\cdot\right)$ are the minimum and maximum matrix eigenvalues, $l_2/l_1 = 1 + \mu\left(\alpha - 1\right)/2 < 1$.

Then we consider the following system:

$$\dot{\boldsymbol{\xi}} = \mathbf{S}_\beta\left(\boldsymbol{\xi}\right) \tag{17}$$

where

$$\mathbf{S}_\beta\left(\boldsymbol{\xi}\right) = \begin{bmatrix}-g_1\omega_0\mathbf{Sig}^{\beta_1}\left(\boldsymbol{\xi}_1\right)\\ -g_2\omega_0\mathbf{Sig}^{\beta_2}\left(\boldsymbol{\xi}_1\right)\\ -g_3\omega_0\mathbf{Sig}^{\beta_3}\left(\boldsymbol{\xi}_1\right)\end{bmatrix}. \tag{18}$$

The Lie derivative $L_{S_\beta}V_1\left(\alpha, \boldsymbol{\xi}\right)$ of $V_1\left(\alpha, \boldsymbol{\xi}\right)$ along $\mathbf{S}_\beta\left(\boldsymbol{\xi}\right)$ is homogeneous of degree $l_3 = 2/\mu + 1/\alpha - 1$ with respect to $\mathbf{r}$. Hence, there exists $\kappa_\beta = -\max_{\{\boldsymbol{g}:V_1(\alpha,\boldsymbol{g})=1\}}L_{S_\beta}V_1\left(\alpha, \boldsymbol{g}\right)$ such that

$$L_{S_\beta}V_1\left(\alpha, \boldsymbol{\xi}\right) \le -\kappa_\beta V_1^{l_3/l_1} \tag{19}$$

where $l_3/l_1 = 1 + \mu\left(1/\alpha - 1\right)/2 > 1$.

Finally, the derivative of $V_1\left(\alpha, \boldsymbol{\xi}\right)$ along the estimation error dynamics (12) yields

$$\dot{V}_1\left(\alpha, \boldsymbol{\xi}\right) = L_{S_\alpha}V_1\left(\alpha, \boldsymbol{\xi}\right) + L_{S_\beta}V_1\left(\alpha, \boldsymbol{\xi}\right) + \sum_{i=1}^{n}\frac{\partial V_1}{\partial \xi_{3,i}}\cdot\frac{\gamma_i}{\omega_0^2} \tag{20}$$

where $\partial V_1/\partial\xi_{3,i}$ is homogeneous of degree $l_4 = 2/\mu - 2\alpha + 1$ with respect to $\mathbf{r}$, and the following inequality holds:

$$\kappa_{1,i}V_1^{l_4/l_1} \le \frac{\partial V_1}{\partial \xi_{3,i}} \le \kappa_{2,i}V_1^{l_4/l_1} \tag{21}$$

where $\kappa_{1,i} = \min_{\{\boldsymbol{g}:V_1(\alpha,\boldsymbol{g})=1\}}\partial V_1/\partial\xi_{3,i}$ and $\kappa_{2,i} = \max_{\{\boldsymbol{g}:V_1(\alpha,\boldsymbol{g})=1\}}\partial V_1/\partial\xi_{3,i}$.

According to (16), (19) and (21), we have

$$\dot{V}_1\left(\alpha, \boldsymbol{\xi}\right) \le -\kappa_\alpha V_1^{l_2/l_1} - \kappa_\beta V_1^{l_3/l_1} + \kappa_m\bar{\gamma}V_1^{l_4/l_1}\Big/\omega_0^2 \tag{22}$$

with $\kappa_m = \sum_{i=1}^{n}\max\left\{\left|\kappa_{1,i}\right|, \left|\kappa_{2,i}\right|\right\}$. Then (22) can be rewritten as

$$\begin{aligned}\dot{V}_1\left(\alpha, \boldsymbol{\xi}\right) \le & -\kappa_\alpha V_1^{l_2/l_1} - \kappa_\beta\left(1 - \delta\right)V_1^{l_3/l_1}\\ & - V_1^{l_4/l_1}\left(\kappa_\beta\delta V_1^{l_3/l_1 - l_4/l_1} - \kappa_m\bar{\gamma}/\omega_0^2\right)\end{aligned} \tag{23}$$

where $0 < \delta < 1$ is a positive constant. It is obvious that when $\kappa_\beta\delta V_1^{l_3/l_1 - l_4/l_1} \ge \kappa_m\bar{\gamma}/\omega_0^2$, then $\dot{V}_1\left(\alpha, \boldsymbol{\xi}\right) \le -\kappa_\alpha V_1^{l_2/l_1} - \kappa_\beta\left(1 - \delta\right)V_1^{l_3/l_1}$. According to *Lemma 2*, the estimation error of FxTESO will converge to the following neighborhood around zero:

$$D_1 = \left\{\mathbf{z}\middle|\ \|\mathbf{z}\| \le \sqrt{\bar{V}_1/\lambda_{\min}\left(\mathbf{P}\right)}\right\} \tag{24}$$

where $\bar{V}_1 = \left(\kappa_m\bar{\gamma}/\kappa_\beta\delta\omega_0^2\right)^{l_1/(l_3 - l_4)}$, the settling time T_1 is bounded by

$$T_1 \le T_{\max 1} = \frac{1}{\kappa_\alpha\left(1 - l_2/l_1\right)} + \frac{1}{\kappa_\beta\left(1 - \delta\right)\left(l_3/l_1 - 1\right)}. \tag{25}$$

■

Remark 1 : It is worth noting that $l_1/(l_3 - l_4) > 0$, so $\bar{V}_1$ can be reduced arbitrarily by increasing ω_0.

Remark 2 : According to (24), it can be deduced that $\left|\tilde{x}_{2,i}\right| \le \bar{x}_2 = \omega_0\left(\bar{V}_1/\lambda_{\min}\left(\mathbf{P}\right)\right)^{\frac{\mu\alpha_1}{2}}$, where $\tilde{x}_{2,i}$ is the ith component of $\tilde{\mathbf{x}}_2$.

B. Adaptive Fixed-Time Fault-Tolerant Controller

An adaptive fixed-time fault-tolerant controller is designed to guarantee the actual trajectory $\mathbf{q}$ of manipulator joints track the desired trajectory $\mathbf{q}_d$ within a fixed time.

The sliding surface is designed as

$$\mathbf{s} = \dot{\mathbf{q}}_d - \hat{\mathbf{x}}_2 + \mathbf{H_1}\mathbf{U}^a\left(\mathbf{e}\right) + \mathbf{H}_2\mathbf{Sig}^b\left(\mathbf{e}\right) \tag{26}$$

where $0 < a < 1$, $b > 1$, $\mathbf{s} = \left[s_1, \cdots, s_n\right]^T$, $\mathbf{e} = \mathbf{q}_d - \mathbf{q}$ is the tracking error and $\mathbf{e} = \left[e_1, \ldots, e_n\right]^T$, $\mathbf{H}_1 = \mathrm{diag}\left\{h_{1,1}, \cdots, h_{1,n}\right\}$ and $\mathbf{H}_2 = \mathrm{diag}\left\{h_{2,1}, \cdots, h_{2,n}\right\}$ are parameter matrices, $\mathbf{U}^a\left(\mathbf{e}\right) = \left[u^a\left(e_1\right), \cdots, u^a\left(e_n\right)\right]^T$ with

$$u^a\left(e_i\right) = \begin{cases}\mathrm{sgn}(e_i)|e_i|^a, & |e_i| \ge \sigma\\ \sigma^{a-1}e_i, & |e_i| < \sigma\end{cases} \tag{27}$$

where σ is a small positive constant. The derivative of $\mathbf{s}$ is as follows:

$$\begin{aligned}\dot{\mathbf{s}} &= \ddot{\mathbf{q}}_d - \dot{\hat{\mathbf{x}}}_2 + \left(\mathbf{H_1}\mathbf{F}^a(\mathbf{e}) + \mathbf{H}_2\mathbf{R}^b(\mathbf{e})\right)\dot{\mathbf{e}} \\ &= \ddot{\mathbf{q}}_d - \left(\dot{\mathbf{x}}_2 - \dot{\tilde{\mathbf{x}}}_2\right) + \left(\mathbf{H_1}\mathbf{F}^a(\mathbf{e}) + \mathbf{H}_2\mathbf{R}^b(\mathbf{e})\right)(\dot{\mathbf{q}}_d - \hat{\mathbf{x}}_2) \\ &\quad - \left(\mathbf{H_1}\mathbf{F}^a(\mathbf{e}) + \mathbf{H}_2\mathbf{R}^b(\mathbf{e})\right)\tilde{\mathbf{x}}_2 \\ &= -\mathbf{M}^{-1}(\mathbf{q})\boldsymbol{\tau} - \mathbf{x}_3 + \boldsymbol{\Theta} + \boldsymbol{\Psi}\end{aligned} \tag{28}$$

where $\boldsymbol{\Theta} = \ddot{\mathbf{q}}_d + \left(\mathbf{H_1}\mathbf{F}^a(\mathbf{e}) + \mathbf{H}_2\mathbf{R}^b(\mathbf{e})\right)(\dot{\mathbf{q}}_d - \hat{\mathbf{x}}_2)$, $\boldsymbol{\Psi} = \dot{\tilde{\mathbf{x}}}_2 - \left(\mathbf{H_1}\mathbf{F}^a(\mathbf{e}) + \mathbf{H}_2\mathbf{R}^b(\mathbf{e})\right)\tilde{\mathbf{x}}_2$ and $\boldsymbol{\Psi} = [\psi_1, \cdots, \psi_n]^T$, $\mathbf{R}^b(\mathbf{e}) = \text{diag}\left\{b|e_1|^{b-1}, \cdots, b|e_n|^{b-1}\right\}$, and $\mathbf{F}^a(\mathbf{e}) = \text{diag}\left\{f^a(e_1), \cdots, f^a(e_n)\right\}$ with

$$f^a(e_i) = \begin{cases} a|e_i|^{a-1}, & |e_i| \geq \sigma \\ \sigma^{a-1}, & |e_i| < \sigma \end{cases}. \tag{29}$$

Assumption 2 : The desired trajectory $\mathbf{q}_d$ and its derivatives $\dot{\mathbf{q}}_d$, $\ddot{\mathbf{q}}_d$ are bounded such that $\|\mathbf{q}_d\| \leq \bar{q}_1$, $\|\dot{\mathbf{q}}_d\| \leq \bar{q}_2$, and $\|\ddot{\mathbf{q}}_d\| \leq \bar{q}_3$, where $\bar{q}_1$, $\bar{q}_2$, and $\bar{q}_3$ are unknown positive constants.

Remark 3 : According to FxTESO (11), *Theorem 1*, *Assumption 1 and 2*, we can know that ψ_i and $\tilde{x}_{3,i}$ are bounded, so there exists $|\psi_i| + |\tilde{x}_{3,i}| \leq k_i$, where k_i is an unknown constant.

The adaptive fixed-time fault-tolerant controller is designed as follows:

$$\boldsymbol{\tau} = \mathbf{M}(\mathbf{q})\begin{pmatrix}\hat{\mathbf{K}}\mathbf{tanh}(\mathbf{s}\odot\bar{\mathbf{o}}) + \mathbf{A}_s\mathbf{Sig}^{2m-1}(\mathbf{s}) \\ +\mathbf{B}_s\mathbf{Sig}^{2l-1}(\mathbf{s}) - \hat{\mathbf{x}}_3 + \boldsymbol{\Theta}\end{pmatrix} \tag{30}$$

where $\hat{\mathbf{K}} = \text{diag}\left\{\hat{k}_1, \cdots, \hat{k}_n\right\}$, $\hat{k}_i$ is the estimation of k_i, and the estimation error is $\tilde{k}_i = k_i - \hat{k}_i$, $\mathbf{tanh}(\mathbf{s}\odot\bar{\mathbf{o}}) = [\tanh(s_1/o_1), \cdots, \tanh(s_n/o_n)]^T$, $\bar{\mathbf{o}} = \left[o_1^{-1}\cdots, o_n^{-1}\right]^T$, o_i is design small constant, $\mathbf{A}_s = \text{diag}\{a_{s,1}, \cdots, a_{s,n}\}$ and $\mathbf{B}_s = \text{diag}\{b_{s,1}, \cdots, b_{s,n}\}$ are parameter matrices, $0 < m < 1$, $l > 1$, and $\odot$ represents Hadamard product.

Substituting (30) into (28), we have

$$\begin{aligned}\dot{s}_i = &-\hat{k}_i\tanh(s_i/o_i) - a_{s,i}sig^{2m-1}(s_i) - b_{s,i}sig^{2l-1}(s_i) \\ &- \tilde{x}_{3,i} + \psi_i.\end{aligned} \tag{31}$$

The adaptive law $\hat{k}_i$ is designed as

$$\dot{\hat{k}}_i = \varphi_i\tanh(s_i/o_i)\, s_i - a_{k,i}\hat{k}_i - b_{k,i}\hat{k}_i^{2l-1} \tag{32}$$

where φ_i, $a_{k,i}$, and $b_{k,i}$ are positive parameters. The diagram of the proposed controller is shown in Fig. 1. FxTESO only requires position $\mathbf{q}$ to obtain velocity estimate $\hat{\mathbf{q}}$ and lumped uncertainty estimate $\hat{\mathbf{d}}$. The sliding surface $\mathbf{s}$ is calculated from the desired trajectory $\mathbf{q}_d$, desired velocity $\dot{\mathbf{q}}_d$, and velocity estimate $\hat{\mathbf{q}}$. In addition, the adaptive law $\hat{\mathbf{K}}$, lumped uncertainty estimate $\hat{\mathbf{d}}$, and sliding surface $\mathbf{s}$ are used to generate controller to drive the manipulator.

Theorem 2 : For the manipulator system (1) with actuator partial LOE faults, external disturbances, and unknown nonlinearities, after time T_1, the designed controller (30) with adaptive law (32) can guarantee the sliding surface s_i and the estimation error $\tilde{k}_i$ convergence to a small neighborhood of zero within a fixed time $T_{\max 2}$.

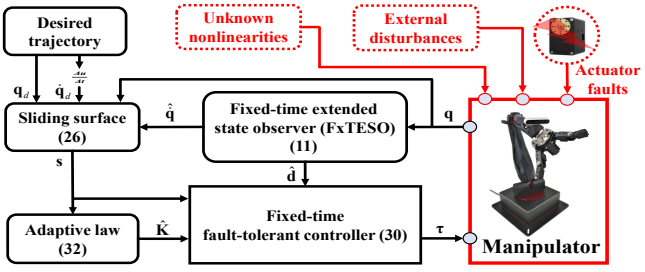

Fig. 1. Diagram of the proposed controller.

Proof: Consider the following Lyapunov function:

$$V_2 = \sum_{i=1}^{n}\frac{s_i^2}{2} + \sum_{i=1}^{n}\frac{\tilde{k}_i^2}{2\varphi_i}. \tag{33}$$

The derivative of V_2 with respect to time is

$$\begin{aligned}\dot{V}_2 = &\sum_{i=1}^{n}\left(-k_i\tanh(s_i/o_i)\, s_i - a_{s,i}|s_i|^{2m} - b_{s,i}|s_i|^{2l}\right) \\ &+ \sum_{i=1}^{n}\left(\frac{a_{k,i}}{\varphi_i}\tilde{k}_i\hat{k}_i + \frac{b_{k,i}}{\varphi_i}\tilde{k}_i\hat{k}_i^{2l-1}\right) \\ &+ \sum_{i=1}^{n}(\psi_i - \tilde{x}_{3,i})\, s_i.\end{aligned} \tag{34}$$

According to $-k_i\tanh(s_i/o_i)\, s_i \leq 0.2785k_io_i - k_i|s_i|$ [19] and *Remark 3*, (34) can be rewritten as

$$\begin{aligned}\dot{V}_2 &\leq \sum_{i=1}^{n}\left(0.2785k_io_i - k_i|s_i| - a_{s,i}|s_i|^{2m} - b_{s,i}|s_i|^{2l}\right) \\ &\quad + \sum_{i=1}^{n}\left(\frac{a_{k,i}}{\varphi_i}\tilde{k}_i\hat{k}_i + \frac{b_{k,i}}{\varphi_i}\tilde{k}_i\hat{k}_i^{2l-1} + (|\psi_i| + |\tilde{x}_{3,i}|)|s_i|\right) \\ &\leq \sum_{i=1}^{n}\left(0.2785k_io_i - a_{s,i}|s_i|^{2m} - b_{s,i}|s_i|^{2l}\right) \\ &\quad + \sum_{i=1}^{n}\left(\frac{a_{k,i}}{\varphi_i}\tilde{k}_i\hat{k}_i + \frac{b_{k,i}}{\varphi_i}\tilde{k}_i\hat{k}_i^{2l-1}\right).\end{aligned} \tag{35}$$

The following expression can be obtained by using Young's inequality:

$$\frac{a_{k,i}}{\varphi_i}\tilde{k}_i\hat{k}_i = \frac{a_{k,i}}{\varphi_i}\tilde{k}_ik_i - \frac{a_{k,i}}{\varphi_i}\tilde{k}_i^2 \leq -\frac{a_{k,i}}{2\varphi_i}\tilde{k}_i^2 + \frac{a_{k,i}}{2\varphi_i}k_i^2. \tag{36}$$

Based on *lemma 3*, let $\vartheta = \tilde{k}_i^2\big/2\varphi_i$, $\chi = 1$, $\varsigma = m$, $\iota = 1 - m$ and $\omega = 1/m$, the following inequality holds:

$$\left(\frac{\tilde{k}_i^2}{2\varphi_i}\right)^m - (1-m)\, m^{\frac{m}{1-m}} \leq \frac{\tilde{k}_i^2}{2\varphi_i}. \tag{37}$$

If the initial value of $\hat{k}_i$ satisfies $\hat{k}_i(0) \geq 0$, then $\hat{k}_i(t) \geq 0, \forall t \geq 0$ [18], and according to *lemma 4*, we have

$$\tilde{k}_i\hat{k}_i^{2l-1} = \tilde{k}_i\left(k_i - \tilde{k}_i\right)^{2l-1} \leq \frac{(2l-1)}{2l}\left(k_i^{2l} - \tilde{k}_i^{2l}\right). \tag{38}$$

Substituting (36), (37) and (38) into (35) yields

$$\begin{aligned}\dot{V}_2 \le & -\sum_{i=1}^{n} a_{s,i}2^m\left(\frac{s_i^2}{2}\right)^m - \sum_{i=1}^{n} a_{k,i}\left(\frac{\tilde{k}_i^2}{2\varphi_i}\right)^m \\ & - \sum_{i=1}^{n} b_{s,i}2^l\left(\frac{s_i^2}{2}\right)^l - \sum_{i=1}^{n}\frac{2l-1}{l}b_{k,i}(2\varphi_i)^{l-1}\left(\frac{\tilde{k}_i^2}{2\varphi_i}\right)^l \\ & + \sum_{i=1}^{n}\left(0.2785k_io_i + a_{k,i}(1-m)\,m^{\frac{m}{1-m}}\right) \\ & + \sum_{i=1}^{n}\left(\frac{a_{k,i}k_i^2}{2\varphi_i} + \frac{b_{k,i}}{\varphi_i}\frac{2l-1}{2l}k_i^{2l}\right).\end{aligned} \tag{39}$$

Then (39) can be simplified to the following form

$$\begin{aligned}\dot{V}_2 \le & -\hbar\left(\sum_{i=1}^{n}\left(\frac{s_i^2}{2}\right)^m + \sum_{i=1}^{n}\left(\frac{\tilde{k}_i^2}{2\varphi_i}\right)^m\right) \\ & -\lambda\left(\sum_{i=1}^{n}\left(\frac{s_i^2}{2}\right)^l + \sum_{i=1}^{n}\left(\frac{\tilde{k}_i^2}{2\varphi_i}\right)^l\right) + \eta\end{aligned} \tag{40}$$

where

$$\begin{aligned}\hbar &= \min_{1\le i\le n}\left\{a_{s,i}2^m, a_{k,i}\right\}, \\ \lambda &= \min_{1\le i\le n}\left\{b_{s,i}2^l, \frac{b_{k,i}(2l-1)}{l}(2\varphi_i)^{l-1}\right\}, \\ \eta &= \sum_{i=1}^{n}\left(0.2785k_io_i + a_{k,i}(1-m)\,m^{\frac{m}{1-m}}\right) \\ &\quad + \sum_{i=1}^{n}\left(\frac{a_{k,i}k_i^2}{2\varphi_i} + \frac{b_{k,i}}{\varphi_i}\frac{2l-1}{2l}k_i^{2l}\right).\end{aligned} \tag{41}$$

According to *lemma 5*, it can be obtained that

$$\begin{aligned}\dot{V}_2 &\le -\hbar\left(\sum_{i=1}^{n}\frac{s_i^2}{2} + \sum_{i=1}^{n}\frac{\tilde{k}_i^2}{2\varphi_i}\right)^m \\ &\quad -\lambda(2n)^{1-l}\left(\sum_{i=1}^{n}\frac{s_i^2}{2} + \sum_{i=1}^{n}\frac{\tilde{k}_i^2}{2\varphi_i}\right)^l + \eta \\ &= -\hbar V_2^m - \ell V_2^l + \eta\end{aligned} \tag{42}$$

where $\ell = \lambda(2n)^{1-l}$.

It can be derived from (42) and *Lemma 2*, the sliding surface s_i and the estimation error $\tilde{k}_i$ converge to a small set around origin within a fixed time, and the set is define as

$$\begin{aligned}D_2 &= \left\{\left(s_i, \tilde{k}_i\right)|V_2 \le \bar{V}_2\right\}, \\ \bar{V}_2 &= \min\left\{\left(\frac{\eta}{(1-\phi)\hbar}\right)^{\frac{1}{m}}, \left(\frac{\eta}{(1-\phi)\ell}\right)^{\frac{1}{l}}\right\}\end{aligned} \tag{43}$$

where $0<\phi<1$, and the settling time T_2 satisfies

$$T_2 \le T_{\max 2} = \frac{1}{\hbar\phi(1-m)} + \frac{1}{\ell\phi(l-1)}. \tag{44}$$

■

Remark 4 : Define a constant $\varpi = \sqrt{2\bar{V}_2}$, it is obvious that $|s_i| \le \varpi$ and $e_is_i \le \varpi|e_i|$.

Theorem 3 : After the sliding surface s_i converges to D_2, the tracking error e_i satisfies

(I) If $|e_i| \ge \sigma$, e_i will converge to a small neighborhood D_3 of the origin within a fixed time $T_{\max 3}$, and

$$\begin{aligned}D_3 &= \{e_i||e_i| \le \Xi_i\}, \\ \Xi_i &= \min\left\{\left(\frac{\varpi+\bar{x}_2}{(1-\upsilon)h_{1,i}}\right)^{\frac{1}{a}}, \left(\frac{\varpi+\bar{x}_2}{(1-\upsilon)h_{2,i}}\right)^{\frac{1}{b}}\right\}\end{aligned} \tag{45}$$

where $0<\upsilon<1$.

(II) If $|e_i| < \sigma$ and $h_{1,i}\sigma^{a-1}|e_i| + h_{2,i}|e_i|^b \ge \varpi + \bar{x}_2$, e_i will converge to a neighborhood D_4 of the origin and

$$D_4 = \left\{e_i|h_{1,i}\sigma^{a-1}|e_i| + h_{2,i}|e_i|^b \le \varpi + \bar{x}_2\right\}. \tag{46}$$

Proof: (I) $|e_i| \ge \sigma$: From *Theorem 2* and (27), it can be inferred that

$$s_i = \dot{e}_i + \tilde{x}_{2,i} + h_{1,i}\,\mathrm{sgn}(e_i)|e_i|^a + h_{2,i}\,\mathrm{sgn}(e_i)|e_i|^b \le \varpi. \tag{47}$$

Multiplying (47) by e_i yields

$$e_i\dot{e}_i + h_{1,i}|e_i|^{a+1} + h_{2,i}|e_i|^{b+1} \le (\varpi+\bar{x}_2)|e_i|. \tag{48}$$

Consider the candidate Lyapunov function $V_3 = e_i^2/2$. Combining (48), the time derivative of V_3 is

$$\begin{aligned}\dot{V}_3 &= e_i\dot{e}_i \\ &\le -h_{1,i}|e_i|^{a+1} - h_{2,i}|e_i|^{b+1} + (\varpi+\bar{x}_2)|e_i| \\ &= -h_{1,i}2^{\frac{a+1}{2}}\left(\frac{e_i^2}{2}\right)^{\frac{a+1}{2}} - h_{2,i}2^{\frac{b+1}{2}}\left(\frac{e_i^2}{2}\right)^{\frac{b+1}{2}} \\ &\quad + (\varpi+\bar{x}_2)|e_i| \\ &= -h_{1,i}2^{\frac{a+1}{2}}(V_3)^{\frac{a+1}{2}} - h_{2,i}2^{\frac{b+1}{2}}(V_3)^{\frac{b+1}{2}} + (\varpi+\bar{x}_2)|e_i|.\end{aligned} \tag{49}$$

According to *Lemma 2*, e_i will converge to D_3 within the following fixed time:

$$T_3 \le T_{\max 3} = \frac{1}{h_{1,i}2^{\frac{a+1}{2}}\upsilon\left(1-\frac{a+1}{2}\right)} + \frac{1}{h_{2,i}2^{\frac{b+1}{2}}\upsilon\left(\frac{b+1}{2}-1\right)}. \tag{50}$$

(II) $|e_i| < \sigma$: From *Theorem 2* and (27), we have

$$e_i\dot{e}_i + h_{1,i}\sigma^{a-1}e_i^2 + h_{2,i}|e_i|^{b+1} \le (\varpi+\bar{x}_2)|e_i| \tag{51}$$

then the derivative of V_3 is

$$\dot{V}_3 = e_i\dot{e}_i \le -h_{1,i}\sigma^{a-1}e_i^2 - h_{2,i}|e_i|^{b+1} + (\varpi+\bar{x}_2)|e_i|. \tag{52}$$

If $h_{1,i}\sigma^{a-1}|e_i| + h_{2,i}|e_i|^b \ge \varpi + \bar{x}_2$, then $\dot{V}_3 \le 0$, and e_i will eventually converge to the domain D_4.

■

Remark 5 : According to *Theorem 1, 2* and *3*, the total time for $|e_i|$ to converge to D_3 satisfies $T \le T_{\max} = T_{\max 1} + T_{\max 2} + T_{\max 3}$.

TABLE I

PARAMETERS OF EACH CONTROLLER

Controller	Parameters
PID	$\mathbf{K}_p = \text{diag}\{65, 150, 65, 25\}$, $\mathbf{K}_I = \text{diag}\{1, 5, 1, 0.5\}$, $\mathbf{K}_D = \text{diag}\{0.5, 5, 1, 0.5\}$.
NFTSMC	$h = 2$, $a = 5$, $b = 3$, $\bar{\Delta} = 400$, $\bar{\eta} = 1$, $\mathbf{K}_1 = \text{diag}\{170, 40, 190, 120\}$, $\mathbf{K}_2 = \text{diag}\{30, 5, 25, 15\}$.
Proposed	$\omega_0 = 200$, $g_1 = 3$, $g_2 = 3$, $g_3 = 1$, $\alpha = 0.95$, $a = 0.9$, $b = 1.1$, $\sigma = 0.001$, $m = 0.9$, $l = 3$, $\mathbf{H}_1 = \mathbf{I}_4$, $\mathbf{H}_2 = 2\mathbf{I}_4$, $\mathbf{A}_s = \text{diag}\{1, 2, 10, 1\}$, $\mathbf{B}_s = 2\mathbf{I}_4$, $o_i = 0.1$, $\varphi_i = 50$, $a_{k,i} = 2$, $b_{k,i} = 1$ $(i = 1, \cdots, 4)$.

IV. EXPERIMENTAL VERIFICATION

This paper verifies the performance of the proposed controller on the Quanser's QArm manipulator, which consists of 4-DOF joints (Q1-Q4, roll-pitch-pitch-roll configuration), and only the motions of Q2 and Q3 are considered in this paper. The control algorithm is developed in Matlab/Simulink environment with the QUARC library. The dynamic model of the QArm and more details can be found in [20]. The experimental platform of QArm is shown in Fig. 4.

A. The Performance of Fault Tolerance and Disturbance Rejection

Different actuator partial LOE faults and external disturbances are imposed on Q2 and Q3, the desired trajectory is $q_{d,2} = q_{d,3} = \sin(2\pi t/15)$ rad, and the duration of all experiments is 105 s. In 20-30 s, the joint Q2 is subjected to an external disturbance of $\tau_{d,2} = 1.06\sin(\pi t)$ N·m. In 40-50 s, the joint Q3 is subjected to an external disturbance of $\tau_{d,3} = 0.53\sin(\pi t)$ N·m. In addition, Q2 and Q3 undergo actuator partial LOE faults with $\lambda_2 = 0.5$ at 60 s and $\lambda_3 = 0.6$ at 70 s respectively. The initial values of the FxTESO and controller are zero.

The experimental results of the PID controller and the NFTSMC controller [6] are also compared to further demonstrate the superiority of the proposed controller. The sliding surface of the NFTSMC controller is

$$\mathbf{s}_N = \mathbf{e} + \mathbf{K}_1 \mathbf{Sig}^h(\mathbf{e}) + \mathbf{K}_2 \mathbf{Sig}^{\frac{a}{b}}(\dot{\mathbf{e}}) \tag{53}$$

where $\mathbf{K}_1$ and $\mathbf{K}_2$ are two gain matrices, a and b are positive odd numbers and satisfy $1 < a/b < 2$ and $h > a/b$.

The NFTSMC controller is designed as

$$\begin{aligned}
&\boldsymbol{\tau} = \boldsymbol{\tau}_{eq} + \boldsymbol{\tau}_{re},\\
&\boldsymbol{\tau}_{eq} = \mathbf{M}\left(\begin{array}{l}\frac{b}{a}\mathbf{K}_2^{-1}\mathbf{Sig}^{\left(2-\frac{a}{b}\right)}(\dot{\mathbf{e}}) - \mathbf{M}^{-1}(-\mathbf{C}\dot{\mathbf{q}} - \mathbf{G}) + \\ \ddot{\mathbf{q}}_d + \frac{b}{a}h\mathbf{K}_2^{-1}\mathbf{K}_1 \text{diag}\left\{|e_i|^{h-1}\right\}\mathbf{Sig}^{\left(2-\frac{a}{b}\right)}(\dot{\mathbf{e}})\end{array}\right),\\
&\boldsymbol{\tau}_{re} = \mathbf{M}\left(\bar{\Delta} + \bar{\eta}\right)\mathbf{tanh}(\mathbf{s}_N)
\end{aligned} \tag{54}$$

where $\bar{\eta}$ is a small positive constant, $\bar{\Delta}$ is an upper bound and $\bar{\Delta} \geq \left\|\mathbf{M}^{-1}\left((\boldsymbol{\Lambda} - \mathbf{I}_4)\boldsymbol{\tau} - \mathbf{F} - \boldsymbol{\tau}_d - \boldsymbol{\Delta}\right)\right\|$. The parameters of all controllers are given in Table I.

The tracking trajectories and corresponding errors of joints Q2 and Q3 are shown in Fig. 2, and the estimations of uncertainties $d_2(t)$ and $d_3(t)$ are shown in Fig. 3. As can be seen from Fig. 2, the proposed fixed-time fault-tolerant controller based on FxTESO has the highest tracking accuracy under any conditions. After Q2 and Q3 are subject to external disturbances, FxTESO can estimate them in real time as shown in Fig. 3, and their negative effects on the system are compensated. However, the performance of both

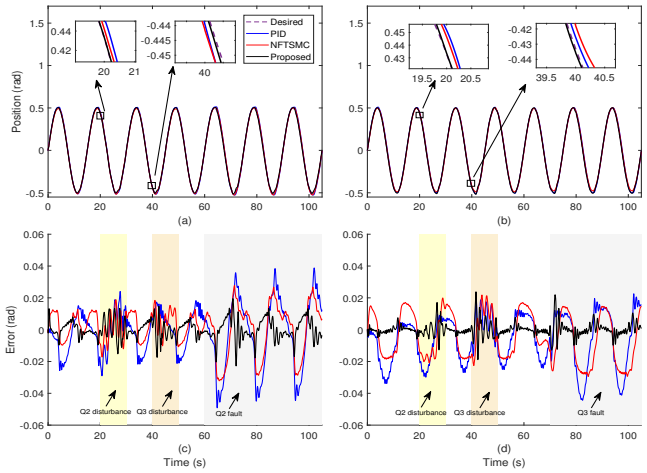

Fig. 2. Tracking trajectories and corresponding errors of Q1 and Q2 with different controllers. (a) Tracking trajectories of Q2. (b) Tracking trajectories of Q3. (c) Tracking errors of Q2. (d) Tracking errors of Q3.

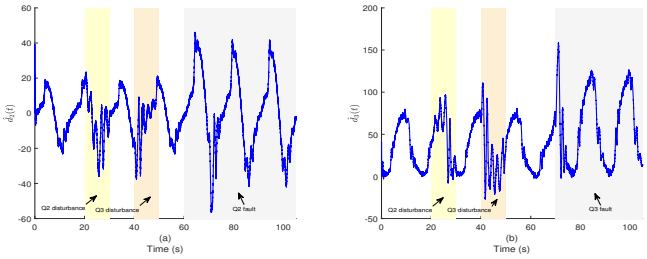

Fig. 3. (a) Estimate of $d_2(t)$. (b) Estimate of $d_3(t)$.

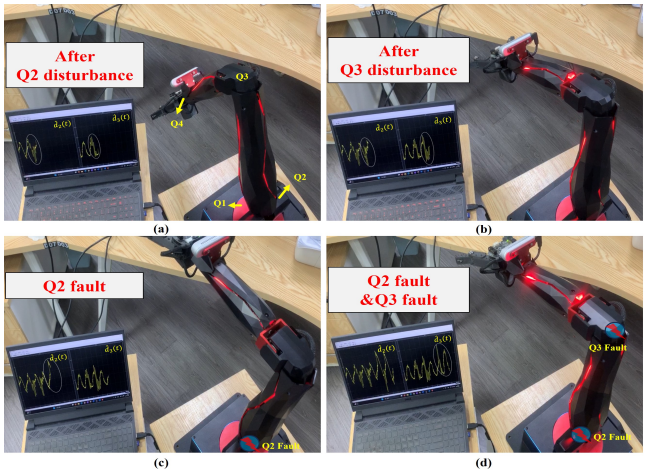

Fig. 4. Experimental scene and real-time signal display. (a) After Q2 disturbance and before Q3 disturbance. (b) After Q3 disturbance and before Q2 fault. (c) After Q2 fault and before Q3 fault. (d) After Q3 fault.

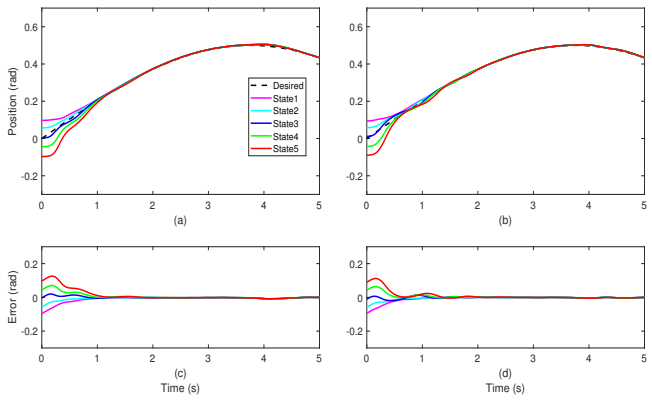

Fig. 5. Tracking trajectories and corresponding errors of Q1 and Q2 under five different initial conditions. (a) Tracking trajectories of Q2. (b) Tracking trajectories of Q3. (c) Tracking errors of Q2. (d) Tracking errors of Q3.

the PID controller and the NFTSMC controller becomes significantly worse after external disturbances. In addition, from Fig. 3, after the actuator faults occur in Q2 at 60 s and in Q3 at 70 s, due to the appearance of fault components $\mathbf{M}^{-1}(\mathbf{q})(\mathbf{\Lambda}-\mathbf{I}_4)\boldsymbol{\tau}$ in the lumped uncertainty $\mathbf{d}(t)$, the estimated values of $d_2(t)$ and $d_3(t)$ increased accordingly to compensate for the faults. We can also see from Fig. 2 that after the occurrence of faults, the proposed controller still has the minimum tracking error, and the performance after the faults remains similar to that before the faults. However, the performance of the PID and NFTSMC controllers significantly deteriorate after the faults, with tracking errors much larger than those of the proposed controller. The experimental scene and the real-time signal display of $\hat{d}_2(t)$ and $\hat{d}_3(t)$ are shown in Fig. 4.

B. The Performance of Fixed-Time Convergence

To verify the fixed-time convergence performance of the proposed controller, experiments are conducted with Q2 and Q3 at five different initial positions, defined as state1-state5 (0.1, 0.05, 0, -0.05, -0.1) rad. The tracking trajectories and corresponding errors of all states are shown in Fig. 5. It can be seen that the tracking errors of the manipulator joints Q2 and Q3 can achieve fixed-time convergence, with the settling time independent of the initial conditions.

V. Conclusion

In this paper, a fixed-time fault-tolerant controller based on FxTESO is proposed for n-DOF manipulators, which considers the existence of actuator partial LOE faults, external disturbances, and unknown nonlinearities. The tracking error of each joint can converge to a neighborhood of zero within a fixed time, and the settling time is independent of the initial conditions. A FxTESO is designed to estimate joint velocities and lumped uncertainty, and an adaptive law is designed to estimate an upper bound associated with the FxTESO error to enhance the controller robustness. The proposed controller requires no prior knowledge about lumped uncertainty, and the estimated velocities is used in controller design, which avoids the significant noise caused by differentiating the position signal. The comparative experimental results with PID and NFTSMC controllers demonstrate the excellence of the proposed controller.

References

[1] C. Jing, H. Xu, and X. Niu, "Adaptive sliding mode disturbance rejection control with prescribed performance for robotic manipulators," *ISA Trans.*, vol. 91, pp. 41–51, 2019.

[2] Y. Wu, R. Huang, X. Li, and S. Liu, "Adaptive neural network control of uncertain robotic manipulators with external disturbance and time-varying output constraints," *Neurocomputing*, vol. 323, pp. 108–116, 2019.

[3] B. Xiao and S. Yin, "Exponential tracking control of robotic manipulators with uncertain dynamics and kinematics," *IEEE Trans. Ind. Inform.*, vol. 15, no. 2, pp. 689–698, 2019.

[4] M. Van and S. S. Ge, "Adaptive fuzzy integral sliding-mode control for robust fault-tolerant control of robot manipulators with disturbance observer," *IEEE Trans. Fuzzy Syst.*, vol. 29, no. 5, pp. 1284–1296, 2021.

[5] F. Zhang, W. Wu, R. Song, and C. Wang, "Dynamic learning-based fault tolerant control for robotic manipulators with actuator faults," *J. Franklin Inst.*, vol. 360, no. 2, pp. 862–886, 2023.

[6] M. Van, S. S. Ge, and H. Ren, "Finite time fault tolerant control for robot manipulators using time delay estimation and continuous nonsingular fast terminal sliding mode control," *IEEE Trans. Cybern.*, vol. 47, no. 7, pp. 1681–1693, 2017.

[7] A. Polyakov, "Nonlinear feedback design for fixed-time stabilization of linear control systems," *IEEE Trans. Autom. Control*, vol. 57, no. 8, pp. 2106–2110, 2012.

[8] C. Zhu, Y. Jiang, and C. Yang, "Fixed-time neural control of robot manipulator with global stability and guaranteed transient performance," *IEEE Trans. Ind. Electron.*, vol. 70, no. 1, pp. 803–812, 2023.

[9] Y. Liu, H. Zhang, Y. Wang, and S. Yu, "Fixed-time cooperative control for robotic manipulators with motion constraints using unified transformation function," *Int. J. Robust Nonlinear Control*, vol. 31, no. 14, pp. 6826–6844, 2021.

[10] S. Cao, L. Sun, J. Jiang, and Z. Zuo, "Reinforcement learning-based fixed-time trajectory tracking control for uncertain robotic manipulators with input saturation," *IEEE Trans. Neural Netw. Learn. Syst.*, vol. 34, no. 8, pp. 4584–4595, 2023.

[11] M. Van and D. Ceglarek, "Robust fault tolerant control of robot manipulators with global fixed-time convergence," *J. Franklin Inst.*, vol. 358, no. 1, pp. 699–722, 2021.

[12] L. Zhang, H. Liu, D. Tang, Y. Hou, and Y. Wang, "Adaptive fixed-time fault-tolerant tracking control and its application for robot manipulators," *IEEE Trans. Ind. Electron.*, vol. 69, no. 3, pp. 2956–2966, 2022.

[13] W. Deng and J. Yao, "Extended-state-observer-based adaptive control of electrohydraulic servomechanisms without velocity measurement," *IEEE/ASME Trans. Mechatron.*, vol. 25, no. 3, pp. 1151–1161, 2020.

[14] L. Zhang, C. Wei, R. Wu, and N. Cui, "Fixed-time extended state observer based non-singular fast terminal sliding mode control for a vtvl reusable launch vehicle," *Aerosp. Sci. Technol.*, vol. 82, pp. 70–79, 2018.

[15] W. Perruquetti, T. Floquet, and E. Moulay, "Finite-time observers: application to secure communication," *IEEE Trans. Autom. Control,*, vol. 53, no. 1, pp. 356–360, 2008.

[16] D. Ba, Y.-X. Li, and S. Tong, "Fixed-time adaptive neural tracking control for a class of uncertain nonstrict nonlinear systems," *Neurocomputing*, vol. 363, pp. 273–280, 2019.

[17] F. Wang and G. Lai, "Fixed-time control design for nonlinear uncertain systems via adaptive method," *Syst. Control Lett.*, vol. 140, p. 104704, 2020.

[18] Y. Sun and L. Zhang, "Fixed-time adaptive fuzzy control for uncertain strict feedback switched systems," *Inf. Sci.*, vol. 546, pp. 742–752, 2021.

[19] X. Jin, "Non-repetitive trajectory tracking for joint position constrained robot manipulators using iterative learning control," in *Proc. IEEE Conf. Decision Control*, 2016, pp. 5490–5495.

[20] Quanser. QARM Product Page. (2023). [Online]. Available: www.quanser.com/products/qarm/.